Supporting Information for:

Photobleaching Kinetics-Based Bead Encoding for Multiplexed Bioassays

Thomas H. Linz†, W. Hampton Henley, and J. Michael Ramsey*

Department of Chemistry

University of North Carolina, Chapel Hill, NC 27599, United States

Histogram Data Processing

A major factor limiting the quality of multiplexed data is the ability to discern different bead populations from one another since misidentified beads can increase error in bioassay measurements. Each population, therefore, has to be characterized to ensure that the identification accuracy is high. For determining identification accuracy in these experiments, chips were loaded with a single bead type and imaged. Fluorescence from each individual bead in the array was measured over time and then normalized to the t=0 value. A histogram was created by sorting the normalized endpoint fluorescence from each individual bead into pre-set bins. Normalized endpoint values reflect the final change in signal after a set duration of photoexposure with a value of 1 representing no change in emission and a value of 0 representing complete loss of signal.

Histograms from each population were compared to determine resolution between populations. Most bins contained beads from a single population although some overlap was observed near the boundaries. Bins containing significant numbers of two bead types (<90% of a single type) were termed “ambiguous” and excluded from the data set to prevent misidentification due to ambiguous bleaching decay values (Figure S1). However, bins containing >90% of one bead type and only a small percentage of another were included, which gave rise to some overlap. Stray beads from one population that fell into the bin of another population were deemed

misidentified. The identification accuracy values reported in this manuscript are the percentages of each bead set that fell in their designated photobleaching bins (i.e. "fast" bin for PE beads, "moderate" bin for Mix beads, and "slow" bin for QD beads). Bin ranges were varied based on the bleaching time to maximize resolution between bead populations. For 1.5 min exposures, histogram bins for the "high" intensity beads were 0.20-0.55, 0.625-0.90, and 0.95-1.30 for "fast", "moderate", and "slow" bins, respectively. The corresponding bin ranges for the "low" intensity beads were 0.3-0.625, 0.70-0.85, and 0.90-1.30, respectively.

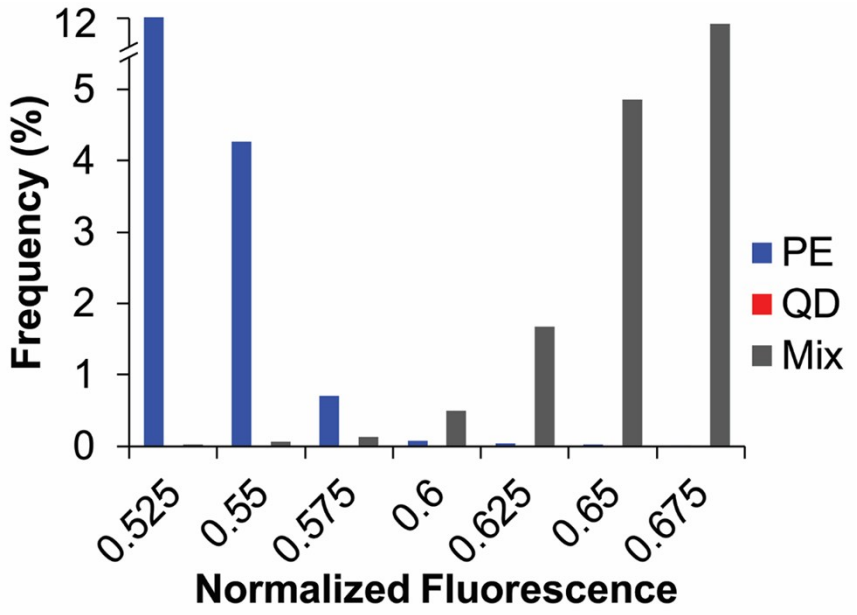

Figure S1. Histogram from "high" encoded beads after 1.5 min of bleaching zoomed in on the overlap region between bead populations. Bins with width 0.025 normalized fluorescence units were created to determine population overlap. Bins 0.575 and 0.6 were excluded from the data set as these bins contained significant amounts (>10%) of both bead populations.

Values listed in Tables 1 and S1 report the data following assignment of individual beads into their designated histogram bins. Since all beads in a population were assigned into bins, the total for each column in the tables sum to 100%. Included in this sum is the percentage of excluded beads for each specific bead population, which is reported throughout this manuscript. However,

to determine the total percentage of beads excluded from an assay, exclusions from each population must be averaged, not added. For example, consider the 1.5 min beads shown in Table S1. It is incorrect to sum the exclusions for PE, Mix, and QD beads as 6.00% + 2.83% + 1.57% = 10.4%. Rather, realize that it is 6.00% of PE beads, 2.83% of Mix beads, and 1.57% of QD beads which are excluded. Assuming a 1:1:1 ratio of each population, the total exclusion is 3.47%.

Encoding accuracy is determined from the rows of Tables 1 and S1, where the percentages of each bead population within a bleaching bin sum to an arbitrary percentage. To obtain encoding accuracy values, the number of beads that fell in their designated photobleaching bins were normalized to the total number of beads within that bin. For example, consider the Fast bin for the 1.5 min bleached beads in Table S1. It can be seen that 93.86% of PE beads, 0.26% of Mix beads, and 0.00% of QD beads fall within that bin. Because the Fast bin is designated for PE beads, the encoding accuracy is calculated as the number of PE beads relative to the total number of beads. In this case, 93.86 ÷ (93.86 + 0.26 + 0.00) which equals the 99.7% accuracy reported below.

Characterization of "Low" Intensity Beads

Photobleaching measurements were obtained for the "low" intensity bead populations in a manner analogous to the "high" intensity beads described in the main text. Each population showed the same characteristic bleaching profile specific to the dye(s) used to encode them (Figure 2a). Figure S2 illustrates this decay from the three bead sets with five replicate chips shown for each. The high precision of the dynamic decoding method is evidenced by the traces essentially overlying one another.

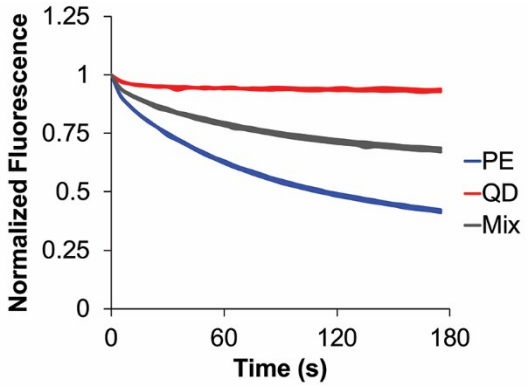

Figure S2. Photobleaching decay profiles of the "low" intensity level beads. Beads were encoded with PE, QDs, or a Mix of both dyes. Average data from five replicate chips (>50k beads) from each bead population are depicted.

Endpoint bleaching decay values for the "low" intensity bead populations were sorted into histograms following a given time of photoexposure (Table S1). It was determined that longer photobleaching times helped increase resolution between the bead populations similar to the "high" intensity beads reported earlier. Again, high identification accuracy was observed for bleaching times ≥1.5 min. Accuracy was not quite as good as with the "high" intensity beads, but was still >99.7% for each bead set after 1.5 min of bleaching, however now with up to 6% of PE beads excluded. Increasing exposure time to 3 min provided >99.98% identification accuracy which was identical to the "high" intensity beads, although 3.3% of PE beads had to be excluded from the analysis due to wider overlap regions between population identification bins.

Table S1. The percentages of beads in each population from the "low" intensity level were sorted into photobleaching bins based on their fluorescence decay. Beads with ambiguous fluorescence values were excluded from the analysis.

Bleaching Bin	0.5 min (%)			1.5 min (%)			3 min (%)		
	PE	Mix	QD	PE	Mix	QD	PE	Mix	QD
Fast	82.14	2.02	0.00	93.86	0.26	0.00	96.70	0.02	0.00
Moderate	0.41	77.51	0.13	0.14	96.89	0.03	0.02	99.13	0.00
Slow	0.00	0.34	92.48	0.00	0.02	98.40	0.00	0.01	99.01
Excluded	17.45	20.13	7.40	6.00	2.83	1.57	3.28	0.84	0.99

Video 1

The attached file contains a sample video illustrating the dynamic decoding process. The microchip area depicted is identical to that in Figure 1 of the manuscript.

Theoretical Encoding States

To determine the hypothetical maximum multiplexing potential of the dynamic encoding approach, Equation 2 was used to determine the total number of encoding states available using five levels of dye at a single wavelength. Each level can be attained by adding appropriate equivalents of one or both dyes to the beads that sum up to the total level value. Figure S3 provides a visual representation of the output. Boxed groups indicate the number of intensity levels achievable, while the subgroups within each box indicate the possible encoding states when incorporating the time domain. Comparing results from "Before" and "After" exposure shows that states can either maintain their current level (if encoded only with stable dye) or decrease in level as a result of bleaching (if encoded with labile dye or a mixture of both). Encoding states, in this iteration, cannot increase in intensity. However, one could envision a process whereby a quencher molecule was released from some of the beads such that sets could move into higher levels. In this

case, additional states could be reached further increasing the multiplexing capacity of the approach.

The benefit of this dynamic encoding technique is illustrated in Figure S4, which plots the ratio of the total number of populations available between dynamic and static encoded states ($T_{Dynamic}/T_{Static}$) for given intensity levels and imaging bands. In all cases where at least one equivalent of dye is used, $T_{Dynamic}$ is greater than T_{Static}. The increased number of uniquely encoded populations observed scales with each additional intensity level or spectral band incorporated into the method. In the example of five intensity levels with three imaging bands, there are 43-fold more populations available with dynamic encoding than possible with the conventional static imaging approach.

	Before		After	
Level	Stable	Labile	Stable	Labile
5	5	0		
	4	1		
	3	2	5	0
	2	3		
	1	4		
	0	5		
4	4	0		
	3	1	4	1
	2	2	4	0
	1	3		
	0	4		
3	3	0	3	2
	2	1	3	1
	1	2	3	0
	0	3		
2			2	3
	2	0	2	2
	1	1	2	1
	0	2	2	0
1			1	4
			1	3
	1	0	1	2
	0	1	1	1
			1	0
0			0	5
			0	4
	0	0	0	3
			0	2
			0	1
			0	0

Figure S3. A schematic of a quantized approach to time-domain encoding where two dyes with spectral overlap and different stabilities are mixed to achieve five distinguishable fluorescence intensity levels. By observing how the "Before" intensity levels change after exposure, 21 different types of uniquely encoded beads can be obtained for a single excitation/emission band due to unique mapping of before and after intensity levels for each bead type. Note that the

position in the “After” column is determined solely by the quantity of “stable” dye used to encode the bead.

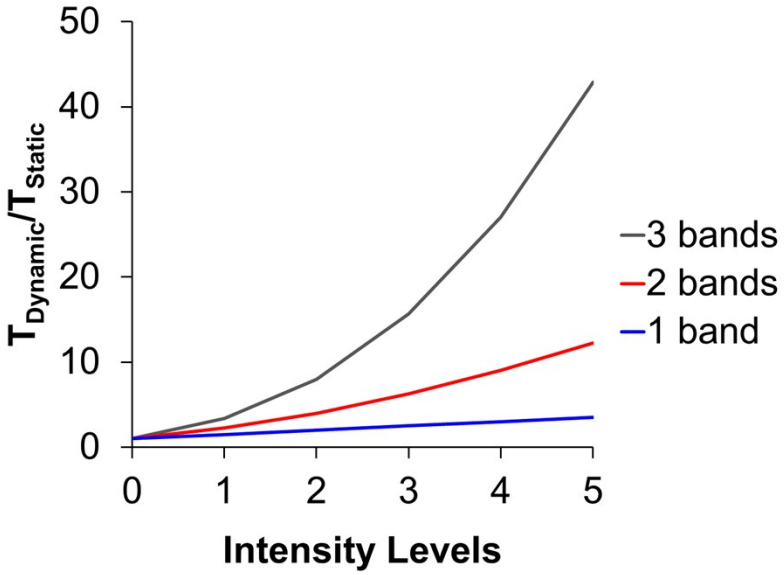

Figure S4. The ratio of $T_{Dynamic}$ to T_{Static} illustrates the benefit of introducing the time domain into encoding measurements. The number of uniquely encoded populations is greater with dynamic decoding for all non-zero intensity levels, and increases sharply when additional spectral bands are introduced.